



Kohn-Luttinger correction to T_c in a phonon superconductorDan Phan  and Andrey V. Chubukov *School of Physics and Astronomy, University of Minnesota, Minneapolis, Minnesota 55455, USA*

(Received 10 October 2019; revised manuscript received 27 November 2019; published 6 January 2020)

Weak coupling theory predicts the critical temperature of a phonon superconductor to be $T_c = 1.13e^{-3/2}\omega_D e^{-1/\lambda}$, where ω_D is the Debye frequency, λ is the dimensionless electron-phonon coupling constant, and the factor $e^{-3/2}$ comes from fermionic self-energy and frequency dependence of the interaction. Other corrections are small either in ω_D/E_F , by Migdal's theorem, or in λ . However, this formula assumes that $\omega_D \ll E_F$, where E_F is the Fermi energy. We obtain T_c in the dilute regime, when the Fermi energy is smaller than ω_D . We argue that in this situation Migdal's theorem is no longer valid, and Kohn-Luttinger-type corrections to the pairing interaction must be included to obtain the correct prefactor for T_c .

DOI: [10.1103/PhysRevB.101.024503](https://doi.org/10.1103/PhysRevB.101.024503)**I. INTRODUCTION**

This paper is devoted to the calculation of superconducting T_c with the prefactor for phonon-mediated superconductivity in quasi-2D systems at weak coupling, in the small density limit, when the Debye frequency is larger than the Fermi energy.

The BCS theory of phonon-mediated superconductivity [1] predicts the value of superconducting $T_c = 1.13\omega_D e^{-1/\lambda}$. The derivation of this formula uses three approximations. First, the frequency-dependent attraction, mediated by an Einstein phonon with frequency ω_D , is replaced by a constant within a shell of width ω_D around the Fermi surface. Second, a weak coupling is assumed (dimensionless $\lambda \ll 1$) and all corrections of $O(\lambda)$ are neglected. Third, ω_D is assumed to be much smaller than E_F , where E_F is the Fermi energy, and all corrections small in ω_D/E_F are neglected as well.

Subsequent studies have found that $O(\lambda)$ corrections to the exponent in the BCS formula for T_c actually cannot be neglected because they change the prefactor in T_c by a factor $O(1)$.

These corrections were studied in detail in the limit $E_F \gg \omega_D$ for phonon-mediated pairing [2–8] as well as in the more general case involving an arbitrary noncritical bosonic propagator [9].

The corrections were argued to originate from the fermionic self-energy and the frequency dependence of the actual phonon-mediated interaction $V(\omega_m, \omega'_m) \propto \omega_D^2 / [(\omega_m - \omega'_m)^2 + \omega_D^2]$. The self-energy $\Sigma(\omega_m) = i\lambda\omega_m$ changes $1/\lambda$ in the exponent to $(1 + \lambda)/\lambda = 1/\lambda + 1$, which changes the prefactor for T_c by e^{-1} . The frequency dependence of the interaction additionally changes $1/\lambda$ to $(1 + \lambda/2)/\lambda = 1/\lambda + 1/2$, i.e., changes the prefactor by $e^{-1/2}$. The full prefactor of T_c is then $e^{-3/2}$, i.e., with these corrections $T_c = 1.13e^{-3/2}\omega_D e^{-1/\lambda} = 0.252\omega_D e^{-1/\lambda}$. Vertex corrections, which give rise to Kohn-Luttinger (KL)-type renormalization of the pairing vertex, also change the argument of the exponent by $O(\lambda)$. However, in the adiabatic regime where $E_F \gg \omega_D$ these corrections are smaller

by $O(\omega_D/E_F)$ by Migdal's theorem and can be safely neglected.

The goal of this work is to obtain expressions for T_c with accurate prefactors in the situation when the coupling is still weak, but the density of carriers is sufficiently low such that $E_F < \omega_D$. Superconductivity in this limit has attracted high interest in recent years chiefly due to advances in experimental studies of SrTiO₃, where superconductivity is present at carrier densities as low as $n \sim 10^{18} \text{ cm}^{-3}$ [10–12], and in other low-density materials, like Pb_{1-x}Tl_xTe [13], half-Heusler compounds [14], and single-crystal Bi [15]. A full analysis of superconductivity in these systems requires one to analyze the combined effect of phonon-mediated attraction and electron-electron repulsion [10–39]. In this work we consider only the attractive part of the interaction and explicitly compute T_c in the low-density limit. We hope our results can be used as input for future calculations of T_c which include electron-electron interactions.

The limit $E_F \ll \omega_D$ is often associated with Bose-Einstein condensation (BEC) behavior, in which fermions form bound pairs at a pairing instability temperature T_{ins} , which then condense at a smaller T_c . However, in three dimensions (3D), BEC behavior only holds at strong coupling, since there is a threshold on bound state formation. In our study we consider pairing in a quasi-two-dimensional (2D) system where the crossover from BCS to BEC behavior already holds at weak coupling and can be analyzed in a controllable way. We will obtain the pairing instability temperature at weak coupling as a function of the two scales: E_F and $E_0 = \omega_D e^{-2/\lambda}$, which denote the Fermi energy and the bound-state energy of two fermions in vacuum, respectively (note that since we are working at weak coupling, $E_0 \ll \omega_D$). For notational convenience we label this temperature T_c with the understanding that this is the onset temperature for the pairing; the actual superconducting T_c is somewhat smaller due to the destructive effect from phase fluctuations [7,40–42].

Our key results are summarized in Table I and Fig. 5. We obtained expressions for T_c with accurate prefactors in three regimes: $E_F \gg \omega_D$, $\omega_D \gg E_F \gg E_0$, and $E_0 \gg E_F$. In each regime $O(\lambda)$ corrections to the exponent in the

TABLE I. The summary of the analytic results of this paper. The values of corrected T_c include the contributions of the self-energy, the frequency dependence of the pairing vertex, and the dressing of the interaction.

	T_c without corrections	T_c including corrections	$\mu(T_c)$
$\omega_D \ll E_F$	$1.13\omega_D \exp(-1/\lambda)$	$0.25\omega_D \exp(-1/\lambda)$	E_F
$E_0 \ll E_F \ll \omega_D$	$1.13\sqrt{E_F E_0}$	$0.12\sqrt{E_F E_0}$	E_F
$E_F \ll E_0$	$E_0/\log(E_0/E_F)$	$4.48E_0/\log(E_0/E_F)$	$-4.48E_0$

weak-coupling formula for T_c give rise to $O(1)$ numerical factors. At $E_F \gg \omega_D$, these corrections come from fermionic self-energy and from frequency dependence of the interaction, while KL corrections are small in ω_D/E_F and can be neglected. In the other two regimes KL corrections are relevant and must be included to get right prefactor for T_c . In particular, deep in the anti-adiabatic regime, when $E_F \ll E_0 \ll \omega_D$, KL corrections increase the value of T_c . We also compute T_c numerically for values of E_F across these regimes and find good agreement between numerical and analytic results.

That KL corrections to the pairing interaction are relevant at small E_F is not obvious, since these corrections come from the particle-hole channel. At low carrier density, i.e., at small enough E_F , the value of $\mu(T_c)$ is negative. In this situation a particle-hole bubble, taken alone, vanishes because at $\mu(T_c) < 0$ the poles in the two Green's functions in the bubble are in the same half-plane of complex frequency. If the pairing interaction is frequency independent, then all KL-type corrections to the pairing interaction (which here are proportional to particle-hole bubbles) therefore vanish [7,43]. However, our interaction $V_0(\omega_m, \omega'_m) \propto \omega_D^2/[(\omega_m - \omega'_m)^2 + \omega_D^2]$ is dynamical and has poles in both half-planes of frequency. The KL correction to the pairing interaction is a convolution of the two fermionic Green's functions and the dynamical interaction, which does not vanish after frequency integration, even in the limit where E_F approaches 0. To be precise, this statement holds when the bandwidth is much larger than all other energy scales in the problem. For a general bandwidth Λ , the KL correction is a function of Λ/ω_D and E_F/ω_D . In our analysis we assume that $\Lambda \gg \omega_D$. In the opposite limit where $\Lambda \ll \omega_D$, the interaction can be approximated by its static form, and one retrieves previous results [7,43] that KL corrections are irrelevant (see below and Appendix C).

We consider a model of 2D fermions with isotropic dispersion $\varepsilon_k = k^2/2m - \mu$ and effective dynamical

interaction $V_0(\omega_m, \omega'_m) = -g\omega_D^2/[(\omega_m - \omega'_m)^2 + \omega_D^2]$. The dimensionless coupling λ is defined as $\lambda = gN_0$, where $N_0 = m/2\pi$ is the 2D density of states per spin. We follow earlier works [19,39,44] and assume that the RPA-type screening is already included into $V_0(\omega_m, \omega'_m)$. Accordingly, we exclude the screening diagram from KL renormalizations. The resulting contributions to the effective interaction are shown in Fig. 1.

Our work complements several recent mean-field studies of superconductivity at low carrier density in both 3D and quasi-2D systems. The analysis of T_c at $E_F \ll \omega_D$ in quasi-2D systems up to an overall factor has been done in Refs. [7,40,41] and we use the results of these works as an input for our calculations of T_c with the prefactor. In Ref. [45] the authors analyzed the mean-field T_c in a 3D Bardeen-Pines type model with effective phonon-mediated attraction. However, these calculations do not extend to the BEC regime.

In Ref. [46] the authors analyzed the combined effect of electron-electron and electron-phonon interactions at weak coupling, within the mean-field (ladder) approximation and obtained T_c up to a prefactor. Our results pave the way toward extending the work in Ref. [46] to obtain T_c with the accurate prefactor.

References [22,25] computed T_c for a model with electron-electron and electron-phonon interactions within the Eliashberg formalism. This formalism includes self-energy corrections and corrections due to the frequency dependence of the interaction, but neglects KL renormalization of the pairing interaction in the particle-hole channel. Several other works also analyzed superconductivity at low carrier density assuming the system is close to a ferroelectric quantum-critical point [21,32,47]. Here again we argue that KL renormalizations must be included to obtain the onset temperature of the pairing with the exact prefactor.

The paper is organized as follows. In the next section we briefly review mean-field calculations of T_c up to a prefactor at $E_F \gg \omega_D$, $\omega_D \gg E_F \gg E_0$, and $E_0 \gg E_F$. In Sec. III we compute $O(1)$ corrections to T_c from fermionic self-energy and the frequency dependence of the interaction in the three ranges of E_F , and then discuss KL corrections to the pairing interaction. We then combine all $O(1)$ corrections and present the results for the onset temperature of the pairing in the three ranges of E_F . In Sec. IV we present the results of our numerical calculations of T_c . In Sec. V we present our conclusions. In Appendix A we discuss in detail the calculations of the KL corrections in the three regimes $E_F \gg \omega_D$, $E_0 \ll E_F \ll \omega_D$, and $E_F \ll E_0$. In Appendix B we discuss numerical calculations of T_c for a given E_F . Finally, in Appendix C we

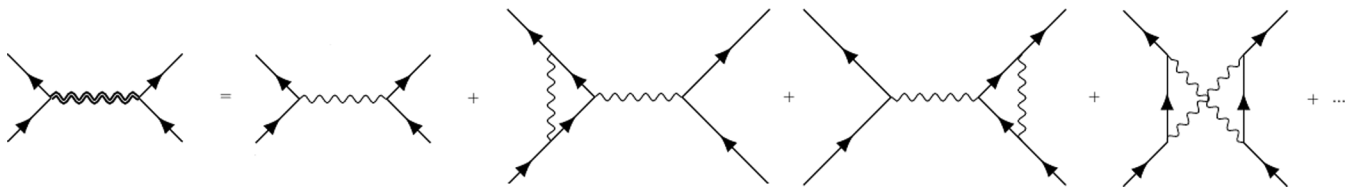


FIG. 1. The diagrammatic expansion of our irreducible pairing interaction (the double wavy line). The single wavy line is the phonon-mediated interaction $V_0(\Omega_m) = -g\omega_D^2/(\Omega_m^2 + \omega_D^2)$. We have ignored conventional screening (a diagram with an internal particle-hole bubble), as this is already included in the bare interaction for our analysis (a screened combined Coulomb and electron-phonon interaction, the attractive part of which is $V_0(\Omega_m)$, see Refs. [16–18,22,23,39,45,46]).

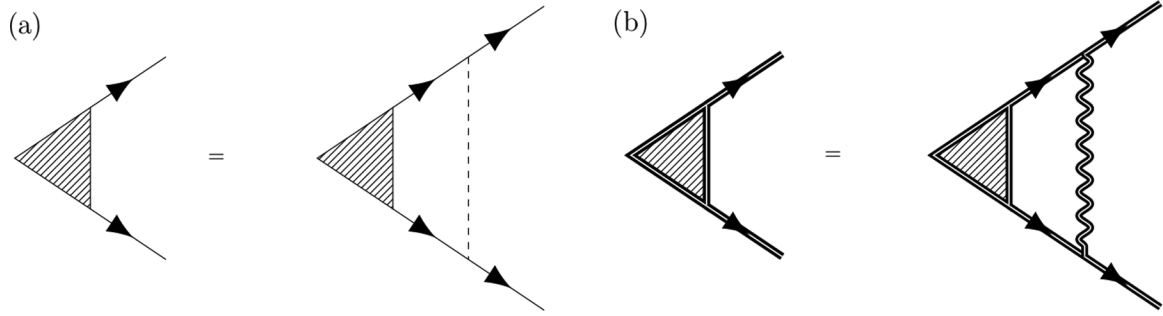


FIG. 2. (a) The equation for the pairing vertex shown diagrammatically, within the BCS approximation. The fermionic Green's functions are bare, and the pairing interaction (dashed line) is treated as a step function. (b) The full equation for the pairing vertex. The Green's functions are fully dressed, and the interaction not only has the correct frequency dependence, but is dressed by Kohn-Luttinger contributions.

discuss how KL corrections get modified for a finite fermionic bandwidth.

II. T_c TO LOGARITHMICAL ACCURACY

In this section we briefly review the derivation of T_c to logarithmical accuracy (i.e., at weak coupling, up to an overall prefactor). We will find that there are three different expressions for T_c for $E_F \gg \omega_D$, $\omega_D \gg E_F \gg E_0$, and $E_0 \gg E_F$.

To obtain T_c to logarithmical accuracy, we begin with the BCS equation for the pairing vertex, shown in Fig. 2(a). Here the phonon-mediated interaction is approximated by a step function $V_0(\Omega_m) = -g\Theta(\omega_D - |\Omega_m|)$. The equation for the pairing vertex therefore becomes

$$\Phi(\omega_m) = gT_c \sum_{\Omega_m} \int \frac{d^2q}{(2\pi)^2} G(q)G(-q) \times \Theta(\omega_D - |\Omega_m - \omega_m|)\Phi(\Omega_m), \quad (2.1)$$

where $G(q) = (i\Omega_m - \varepsilon_q)^{-1}$ is the undressed electronic Green's function, $\varepsilon_q = q^2/2m - \mu(T)$ is the shifted electron energy, and $\mu(T_c)$ is the chemical potential of our system at T_c .

The chemical potential as a function of temperature $\mu(T_c)$ is determined by the constraint of fixed particle number:

$$n = 2T_c \sum_{\omega_m} \int \frac{d^2p}{(2\pi)^2} G(p). \quad (2.2)$$

Upon insertion of the above form of $G(p)$, one obtains an expression for $\mu(T_c)$.

The conventional approximation, valid to logarithmical accuracy (i.e., to leading order in λ), is to take $\Phi(\omega_m)$ as independent of ω_m for $|\omega_m| \ll \omega_D$ and ignore complications at $|\omega_m| \sim \omega_D$. Setting $\Phi(\omega_m) = \Phi$ and canceling it in Eq. (2.1) we obtain

$$1 = gT_c \sum_{\Omega_m} \int \frac{d^2q}{(2\pi)^2} G(q)G(-q)\Theta(\omega_D - |\Omega_m - \omega_m|). \quad (2.3)$$

The simultaneous solution of (2.3) and (2.2) gives T_c and $\mu(T_c)$, which for notational convenience we henceforth label μ_c . Integrating over momentum in Eq. (2.3) and using

$n = 2N_0E_F$, we obtain

$$1 = \lambda T_c \sum_{|\Omega_m| < \omega_D} \frac{1}{|\Omega_m|} \left[\frac{\pi}{2} + \arctan\left(\frac{\mu_c}{|\Omega_m|}\right) \right] \quad (2.4)$$

and

$$\mu_c = T_c \log[\exp(E_F/T_c) - 1], \quad (2.5)$$

where $\lambda = gN_0$. Below we present the solution of Eqs. (2.4) and (2.5) in three ranges of values for E_F . As we will see, $T_c \ll \omega_D$ for all E_F .

A. $E_F \gg \omega_D$

In the range where $E_F \gg \omega_D$, we clearly have $E_F \gg T_c$. Applying this to the formula for the chemical potential, we find $\mu_c \approx E_F$. Hence, $\mu_c/|\Omega_m| > E_F/\omega_D \gg 1$ for all $|\Omega_m| < \omega_D$, and we can safely approximate $\arctan(\mu_c/|\Omega_m|)$ by $\pi/2$. Equation (2.4) then becomes

$$1 = \lambda\pi T_c \sum_{|\Omega_m| < \omega_D} \frac{1}{|\Omega_m|} \quad (2.6)$$

$$= \lambda \log\left(\frac{2e^\gamma \omega_D}{\pi T_c}\right), \quad (2.7)$$

from which we find $T_c = 1.13\omega_D \exp(-1/\lambda)$, the usual BCS result. The sum was done using the Euler-Maclaurin formula, using $T_c \ll \omega_D$.

B. $E_0 \ll E_F \ll \omega_D$

As E_F decreases, we enter the regime where $E_F \ll \omega_D$, but $E_F \gg E_0 \equiv \omega_D \exp(-2/\lambda)$. In this range we will assume and later verify that we still have $\mu_c \approx E_F$, and $T_c \ll E_F$. Equation (2.4) then becomes

$$\frac{1}{\lambda} = \frac{1}{2} \log\left(\frac{2e^\gamma \omega_D}{\pi T_c}\right) + T \sum_{|\Omega_m| < \omega_D} \frac{1}{|\Omega_m|} \arctan\left(\frac{\mu_c}{|\Omega_m|}\right). \quad (2.8)$$

In the second term, it is unnecessary to consider the cutoff at ω_D since the sum converges at $|\Omega_m| \sim \mu_c \ll \omega_D$. The sum can be done using the Euler-Maclaurin formula, and the equation for T_c becomes

$$\frac{1}{\lambda} = \frac{1}{2} \log\left(\frac{2e^\gamma \omega_D}{\pi T_c}\right) + \frac{1}{2} \log\left(\frac{2e^\gamma \mu_c}{\pi T_c}\right). \quad (2.9)$$

Solving for T_c and using $\mu_c \approx E_F$, we find $T_c = 1.13\sqrt{\omega_D E_F} \exp(-1/\lambda) = 1.13\sqrt{E_F E_0}$. Substituting this expression for T_c back into (2.5), we verify that $\mu_c \approx E_F$.

C. $E_F \ll E_0 \ll \omega_D$

As we further decrease E_F , we enter the regime where E_F is much smaller than both E_0 and ω_D . To calculate T_c in this limit, we will assume and then verify that $E_F \ll T_c$ and $|\mu_c| \ll \omega_D$. Using the first assumption, we find $\mu_c \approx T_c \log(E_F/T_c) < 0$ and $|\mu_c| \gg T_c$. Combining this with the second assumption, we have $\omega_D \gg |\mu_c| \gg T_c$. The equation for T_c [Eq. (2.4)] therefore becomes

$$\frac{1}{\lambda} = \frac{1}{2} \log\left(\frac{2e^\gamma \omega_D}{\pi T_c}\right) - T_c \sum_{\Omega_m} \frac{1}{|\Omega_m|} \arctan\left(\frac{|\mu_c|}{\Omega_m}\right) \quad (2.10)$$

$$= \frac{1}{2} \log\left(\frac{2e^\gamma \omega_D}{\pi T_c}\right) - \frac{1}{2} \log\left(\frac{2e^\gamma |\mu_c|}{\pi T_c}\right) \quad (2.11)$$

$$= \frac{1}{2} \log\left(\frac{\omega_D}{|\mu_c|}\right). \quad (2.12)$$

Hence

$$|\mu_c| = \omega_D \exp(-2/\lambda) = E_0, \quad (2.13)$$

and we see that $|\mu_c| \ll \omega_D$, as assumed. Using $|\mu_c| = T_c \log(T_c/E_F)$, we find

$$T_c = \frac{E_0}{\log(E_0/E_F)} \quad (2.14)$$

to leading order in $\log(E_0/E_F)$. This justifies our assumption that $T_c \gg E_F$.

We reiterate that this temperature should be understood to be the pairing instability temperature rather than the actual transition temperature, below which the system develops long-range superconducting order. The latter is smaller due to the destructive effect of phase fluctuations. Though this distinction holds for all values of E_F , it is in this low-density limit that the effect of phase fluctuations is most pronounced.

We also emphasize that Eq. (2.14) is valid only to logarithmic accuracy, i.e., up to numerical prefactors. To get T_c with correct prefactors, one must include all corrections of $O(\lambda)$. This is done in the following section.

III. $O(1)$ CORRECTIONS TO T_c FROM THE SELF-ENERGY, FREQUENCY DEPENDENCE OF THE INTERACTION, AND KL RENORMALIZATIONS

To illustrate the point that $O(1)$ corrections to T_c come from $O(\lambda)$ corrections to BCS theory, consider Eq. (2.6) with an additional term $C\lambda$. We have

$$1 = \lambda \log\left(\frac{2e^\gamma \omega_D}{\pi T_c}\right) + C\lambda \quad (3.1)$$

$$= \lambda \log\left(\frac{2e^\gamma e^C \omega_D}{\pi T_c}\right). \quad (3.2)$$

Solving for T_c we obtain $T_c = \frac{2e^\gamma e^C}{\pi} \omega_D e^{-1/\lambda}$. We see that the exponent $e^{-1/\lambda}$ is unchanged, but the prefactor has been modified by a constant e^C . Hence, terms of order $O(\lambda)$ will

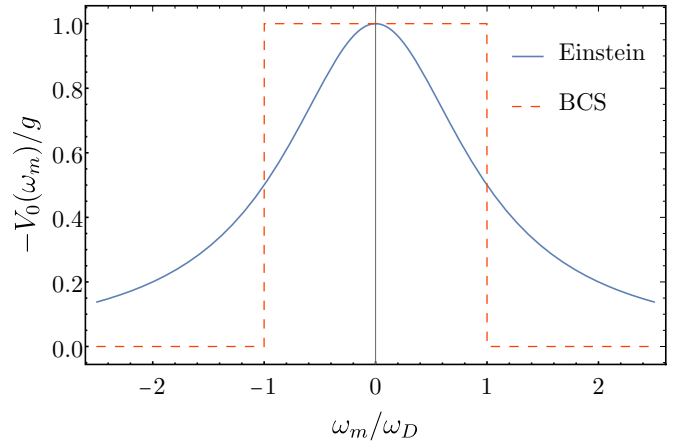


FIG. 3. The Einstein and BCS approximation to the interaction potential, in units of $-g$.

affect the prefactor for T_c . This reasoning applies for all values of E_F .

To take $O(\lambda)$ corrections into account, we write down the linearized equation for the full pairing vertex $\Phi(\omega_m, \mathbf{k})$. It is given diagrammatically by Fig. 2(b). In analytical form we have

$$\begin{aligned} \Phi(\omega_m, \mathbf{k}) = & -T_c \sum_{\Omega_m} \int \frac{d^2 q}{(2\pi)^2} G(\Omega_m, q) G(-\Omega_m, -q) \\ & \times V_{\text{eff}}(\omega_m, \mathbf{k}; \Omega_m, \mathbf{q}) \Phi(\Omega_m, \mathbf{q}), \end{aligned} \quad (3.3)$$

where $G(\Omega_m, q)$ is the Green function for interacting fermions, and $V_{\text{eff}}(\omega_m, \mathbf{k}; \Omega_m, \mathbf{q})$ is the irreducible dynamical interaction in the particle-particle channel, dressed by renormalizations from the particle-hole channel. Equation (3.3) must be solved along with the equation for chemical potential [Eq. (2.5)] with the full fermionic G simultaneously for T_c and μ_c . For our isotropic dispersion, the pairing problem decouples between harmonics with different angular momentum l . Since we are interested in T_c in the s -wave channel, the corresponding pairing vertex is $\Phi(\omega_m, k) = \Phi(\omega_m)$.

In the previous section we approximated $G(\Omega_m, q)$ by its bare value $G_0(\Omega_m, q) = (i\Omega_m - \varepsilon_q)^{-1}$ and the irreducible pairing interaction by a step function $V_0(\omega_m) \rightarrow -g\Theta(\omega_D - |\omega_m|)$. Accordingly, we approximated the s -wave pairing vertex $\Phi(\omega_m)$ by frequency-independent Φ .

To find corrections $O(\lambda)$ we must go beyond these approximations in three different directions:

(1) We must include $O(\lambda)$ renormalization of the electron Green's function $G(\Omega_m, q)$.

(2) We must take into account the frequency dependence of the bare phonon-mediated interaction $V(\Omega_m)$ and solve for the frequency dependent $\Phi(\omega_m)$. The frequency-dependence of the Einstein phonon-mediated interaction is shown in Fig. 3.

(3) We must include KL corrections, which account for the difference between $V_0(\omega_m; \Omega_m)$ and $V_{\text{eff}}(\omega_m, \mathbf{k}; \Omega_m, \mathbf{q})$.

We emphasize that we are only interested in $O(\lambda)$ corrections to the argument in the exponent for T_c —these give rise to $O(1)$ renormalizations of the prefactor for T_c . Accordingly, we neglect regular $O(\lambda)$ corrections to T_c . In the following we

consider each correction individually and later add the results, which is legitimate to $O(\lambda)$.

A. Corrections from the fermionic self-energy

The fermionic self-energy renormalizes the coupling λ into $\lambda^* = \lambda/Z$, where $Z = 1 - id\Sigma(\omega_m)/d\omega_m$. The one-loop self-energy is shown in Fig. 4 and is given by

$$\Sigma(\omega_m, k) = T_c \sum_m \int \frac{d^2q}{4\pi^2} G_0(\Omega_m, q) V_0(\Omega_m - \omega_m), \quad (3.4)$$

where we remind $V_0(\Omega_m) = -g \frac{\omega_D^2}{\omega_D^2 + \Omega_m^2}$. Performing the Matsubara sum, we obtain

$$\begin{aligned} \Sigma(\omega_m, k) = \Sigma(\omega_m) = \frac{\lambda}{2} \omega_D \int_{-\mu_c}^{\infty} d\varepsilon \left(\frac{n_F(\varepsilon) + n_B(\omega_D)}{\varepsilon - i\omega_m - \omega_D} \right. \\ \left. + \frac{1 - n_F(\varepsilon) + n_B(\omega_D)}{\varepsilon - i\omega_m + \omega_D} \right). \end{aligned} \quad (3.5)$$

Because T_c is exponentially small, and $\Sigma(\omega_m)$ already contains λ in the prefactor, the self-energy can be safely approximated by its value at $T = 0$, where $n_F(\varepsilon) = \Theta(-\varepsilon)$ and $n_B(\omega_D) = 0$. We then end up with two expressions, depending on the sign of μ_c .

1. $\mu_c > 0$

Here

$$\begin{aligned} \Sigma(\omega_m) = \Sigma(0) + \frac{\lambda\omega_D}{2} \left[\log \left(\frac{\omega_D + i\omega_m}{\omega_D - i\omega_m} \right) \right. \\ \left. - \log \left(\frac{\mu_c + \omega_D + i\omega_m}{\mu_c + \omega_D} \right) \right]. \end{aligned} \quad (3.6)$$

Because the relevant ω_m are of order T_c , i.e., exponentially smaller than ω_D , one can expand in ω_m . This gives

$$Z = 1 + \frac{\lambda}{2} \frac{2\mu_c + \omega_D}{\mu_c + \omega_D}. \quad (3.7)$$

At $E_F \gg \omega_D$, $\mu_c \approx E_F \gg \omega_D$, and $Z = 1 + \lambda$. This is a well-known result [48]. At $E_0 \ll E_F \ll \omega_D$, we have $\mu_c \approx E_F \ll \omega_D$, and $Z = 1 + \lambda/2$ instead.

2. $\mu_c < 0$

For $\mu_c < 0$, only one of the two integrals survives. Now

$$\Sigma(\omega_m) - \Sigma(0) = \frac{\lambda\omega_D}{2} \log \left(\frac{|\mu_c| + \omega_D}{|\mu_c| + \omega_D - i\omega_m} \right). \quad (3.8)$$

This yields

$$Z = 1 + \frac{\lambda}{2} \frac{\omega_D}{|\mu_c| + \omega_D}. \quad (3.9)$$

Since $|\mu_c| \ll \omega_D$ for negative μ_c , we have $Z = 1 + \lambda/2$.

TABLE II. The summary of the analytic results of this paper regarding modifications to the prefactor of T_c from all corrections of $O(\lambda)$. Also listed is the total correction to the prefactor of T_c , obtained by multiplying the factors from each contribution together.

	$\Sigma(\omega_m)$	$\Phi(\omega_m)$	KL	Total
$\omega_D \ll E_F$	e^{-1}	$e^{-1/2}$	1	$e^{-3/2}$
$E_0 \ll E_F \ll \omega_D$	$e^{-1/2}$	$e^{-1/4}$	$e^{-3/2}$	$e^{-9/4}$
$E_F \ll E_0$	e^{-1}	$e^{-1/2}$	e^3	$e^{3/2}$

Equations (3.6) and (3.8) can be combined into

$$\Sigma(\omega_m) = \Sigma(0) + i\omega_m \frac{\lambda}{2} \frac{|\mu_c| + \mu_c + \omega_D}{|\mu_c| + \omega_D}, \quad (3.10)$$

which holds for both positive and negative μ_c .

With this, we may now derive modified expressions for T_c in all three regimes of E_F , by simply replacing $\lambda \rightarrow \lambda^* = \lambda/Z$ in the expressions for T_c in the previous section. The effect on the prefactor of T_c due to the inclusion of the self-energy in all three cases is summarized in Table II. We recall that $T_c \propto e^{-1/\lambda}$ when $E_F \gg E_0$ and $T_c \propto e^{-2/\lambda}$ when $E_F \lesssim E_0$. In all cases, including the self-energy reduces T_c .

B. Correction to T_c from the frequency dependence of $V_0(\Omega_m)$

Next we obtain the $O(1)$ correction to T_c from the frequency dependence of the electron-phonon interaction $V_0(\Omega_m)$. For $E_F \gg \omega_D$, this has been considered in Refs. [2–6,8,49]. We analyze the correction to T_c in all three regions of E_F . We follow the computational approach used in [8,49].

We start with the Eq. (3.3) for the frequency-dependent pairing vertex at T_c , which we rewrite as

$$\begin{aligned} \Phi(\omega_m) = \frac{\lambda}{N_0} T_c \sum_{\Omega_m} \int \frac{d^2q}{(2\pi)^2} \frac{1}{\Omega_m^2 + \varepsilon_q^2} \frac{\omega_D^2}{\omega_D^2 + (\omega_m - \Omega_m)^2} \\ \times \Phi(\Omega_m). \end{aligned} \quad (3.11)$$

The leading, logarithmical contribution to the r.h.s. of (3.11) comes from small internal Ω_m , for which $\Phi(\Omega_m)/[\omega_D^2 + (\omega_m - \Omega_m)^2] \approx \Phi(0)/(\omega_D^2 + \omega_m^2)$. Accordingly, we search for the solution of (3.11) in the form

$$\Phi(\omega_m) = \Phi(0) \left(\frac{\omega_D^2}{\omega_D^2 + \omega_m^2} + \lambda\delta\Phi(\omega_m) \right). \quad (3.12)$$

We substitute this into (3.11) and set external ω_m to have the smallest possible value, $\omega_m = \pi T_c$. Because T_c is much smaller than typical Ω_m in all three regimes, we can safely neglect $\omega_m = \pi T_c$ compared to Ω_m on the r.h.s. of (3.11). We

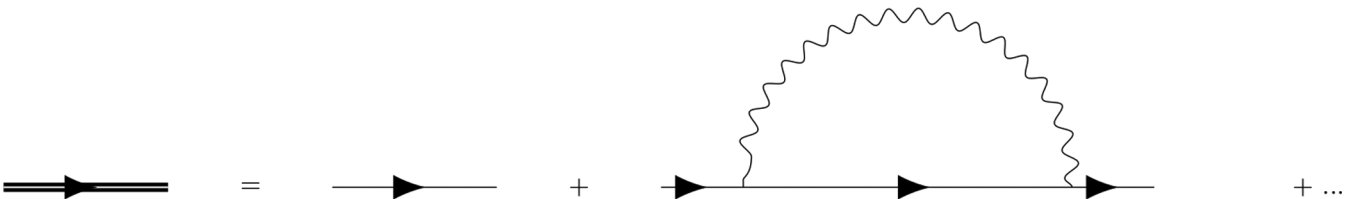


FIG. 4. The fermionic Green's function to first order in the interaction. The tadpole correction (not shown) is already incorporated into μ_c .

find

$$1 + \lambda \delta \Phi(0) = \frac{\lambda}{N_0} T_c \sum_{\Omega_m} \int \frac{d^2 q}{(2\pi)^2} \frac{1}{\Omega_m^2 + \varepsilon_q^2} \frac{\omega_D^2}{\omega_D^2 + \Omega_m^2} \times \left(\frac{\omega_D^2}{\omega_D^2 + \Omega_m^2} + \lambda \delta \Phi(\Omega_m) \right). \quad (3.13)$$

To the same accuracy, the last term on the right-hand side can be approximated as

$$\lambda \delta \Phi(0) I, \quad (3.14)$$

where

$$I = \frac{\lambda}{N_0} T_c \sum_{\Omega_m} \int \frac{d^2 q}{(2\pi)^2} \frac{1}{\Omega_m^2 + \varepsilon_q^2} \frac{\omega_D^2}{\omega_D^2 + \Omega_m^2}. \quad (3.15)$$

One can verify that $I = 1 + O(\lambda)$. Substituting this back into (3.13), we obtain

$$\begin{aligned} & \frac{\lambda}{N_0} T_c \sum_{\Omega_m} \int \frac{d^2 q}{(2\pi)^2} \frac{1}{\Omega_m^2 + \varepsilon_q^2} \left(\frac{\omega_D^2}{\omega_D^2 + \Omega_m^2} \right)^2 \\ &= 1 + \lambda \delta \Phi(0) (1 - I) = 1 + O(\lambda^2). \end{aligned} \quad (3.16)$$

To order $O(\lambda)$ we then have

$$\frac{\lambda}{N_0} T_c \sum_{\Omega_m} \int \frac{d^2 q}{(2\pi)^2} \frac{1}{\Omega_m^2 + \varepsilon_q^2} \left(\frac{\omega_D^2}{\omega_D^2 + \Omega_m^2} \right)^2 = 1. \quad (3.17)$$

Comparing this with Eq. (3.3), we see that the effect of the frequency dependence of the pairing vertex is that $\Theta(\omega_D - |\Omega_m|) \rightarrow [\omega_D^2 / (\omega_D^2 + \Omega_m^2)]^2$. This difference becomes relevant at frequencies comparable to ω_D .

Integrating over momentum in (3.17) we find

$$1 = \lambda T_c \sum_{\Omega_m} \left(\frac{\omega_D^2}{\omega_D^2 + \Omega_m^2} \right)^2 \frac{1}{|\Omega_m|} \left[\frac{\pi}{2} + \arctan \left(\frac{\mu_c}{|\Omega_m|} \right) \right]. \quad (3.18)$$

At $E_F \gg \omega_D$, this reduces to

$$1 = \lambda \pi T_c \sum_{\Omega_m} \left(\frac{\omega_D^2}{\omega_D^2 + \Omega_m^2} \right)^2 \frac{1}{|\Omega_m|} = \log \frac{2e^\gamma \omega_D}{\pi T_c \sqrt{e}}. \quad (3.19)$$

Comparing with T_c in the previous section, we see that T_c is reduced by \sqrt{e} .

For $E_F \ll \omega_D$, recall that the second term on the r.h.s. of Eq. (3.18) converges at $|\Omega_m| \sim |\mu_c| \ll \omega_D$. Therefore, the modification $\Theta(\omega_D - |\Omega_m|) \rightarrow [\omega_D^2 / (\omega_D^2 + \Omega_m^2)]^2$ has no effect on this sum. In this situation, the renormalization factor for T_c comes only from the $\pi/2$ term, and equals $1/e^{1/4}$ instead of $1/\sqrt{e}$. For smaller Fermi energies ($E_F \lesssim E_0$), the only contribution to the renormalization is again from the $\pi/2$ term on the r.h.s. of Eq. (3.18). However, since $T_c \propto e^{-2/\lambda}$, the renormalization factor is $(1/e^{1/4})^2 = 1/\sqrt{e}$.

C. KL renormalization of the pairing interaction

We now take into account the first-order KL correction to the interaction. We express the dressed interaction as $V_{\text{eff}}(\omega_m, k; \omega'_m, k')$ as $V_{\text{eff}}(\omega_m, k; \omega'_m, k') = V_0(\omega_m -$

$\omega'_m) + \lambda \delta V(\omega_m, k; \omega'_m, k') + O(\lambda^2)$. The point of this section is to calculate the effect of $\lambda \delta V(\omega_m, k; \omega'_m, k')$ on T_c . For convenience, we pull out the coupling constant g and express $V_{\text{eff}}(\omega_m, k; \omega'_m, k') = -g D_{\text{eff}}(\omega_m, k; \omega'_m, k')$, where $D_{\text{eff}}(\omega_m, k; \omega'_m, k') = D_0(\omega_m - \omega'_m) + \lambda \delta D(\omega_m, k; \omega'_m, k')$ is dimensionless.

The KL diagrams for $\delta D(\omega_m, k; \omega'_m, k')$ are shown in Fig. 1. There are three first order corrections to the bare interaction. The first two describe vertex corrections, and the third is the exchange (crossing) diagram.

Before calculating $\delta D(\omega_m, k; \omega'_m, k')$ explicitly, we show how it modifies T_c . For this we go back to Eq. (3.3) for the pairing vertex $\Phi(\omega_m, \mathbf{k})$, explicitly express V_{eff} as the sum of the two terms, and neglect other $O(\lambda)$ corrections, i.e., approximate G by its free fermion value and approximate $V(\Omega_m)$ by a step function. The equation for the pairing vertex then reduces to

$$\begin{aligned} \Phi(\omega_m, \mathbf{k}) &= \lambda \frac{T_c}{N_0} \sum_{\Omega_m} \int \frac{d^2 q}{(2\pi)^2} \frac{1}{\Omega_m^2 + \varepsilon_q^2} [\Theta(|\Omega_m - \omega_m| - \omega_D) \\ &+ \lambda \delta D(\omega_m, \mathbf{k}; \Omega_m, \mathbf{q})] \Phi(\Omega_m, \mathbf{q}). \end{aligned} \quad (3.20)$$

Due to the factor of $(\varepsilon_q^2 + \Omega_m^2)^{-1}$, the integrand peaks at $q = k_\mu \equiv \sqrt{2m\mu_c}$ for $\mu_c > 0$ and at $q = 0$ for $\mu_c < 0$. In $\delta D(\omega_m, \mathbf{k}; \Omega_m, \mathbf{q})$ we then set $\mathbf{k} = \mathbf{n}_k k_\mu \Theta(\mu_c)$ and $\mathbf{q} = \mathbf{n}_q k_\mu \Theta(\mu_c)$. Like before, we set $\omega_m = \pi T_c$ and set the pairing vertex to be a nonzero constant for $|\omega_m| < \omega_D$ and 0 for $|\omega_m| > \omega_D$, mirroring the frequency dependence of the bare interaction. We then obtain

$$\begin{aligned} 1 &= \lambda \frac{T_c}{N_0} \sum_{|\Omega_m| < \omega_D} \int \frac{d^2 q}{(2\pi)^2} \frac{1}{\Omega_m^2 + \varepsilon_q^2} \\ &+ \lambda^2 \frac{T_c}{N_0} \sum_{|\Omega_m| < \omega_D} \int \frac{d^2 q}{(2\pi)^2} \frac{1}{\Omega_m^2 + \varepsilon_q^2} \\ &\times \delta D[0, \mathbf{n}_k k_\mu \Theta(\mu_c); \Omega_m, \mathbf{n}_q k_\mu \Theta(\mu_c)]. \end{aligned} \quad (3.21)$$

For the last term there is a logarithmical contribution coming from small frequencies around $\Omega_m = 0$, which cancels one power of λ . Accordingly, we set $\Omega_m = 0$ in δD . Typical momenta are around $q = k_\mu \Theta(\mu_c)$. Thus, when $\mu_c > 0$, these momenta are around the Fermi surface. For $\mu_c < 0$, they are around $q = 0$. Accordingly, for $\mu_c < 0$, we set the momenta in δD to zero. Taking into account finite momenta would lead to additional $O(\lambda^2)$ term on the r.h.s. of (3.21), which we do not need.

The part of the KL interaction relevant for our purposes, is therefore $\delta D[0, \mathbf{n}_k k_\mu \Theta(\mu_c); 0, \mathbf{n}_q k_\mu \Theta(\mu_c)]$. We still need to integrate over the angle between \mathbf{n}_k and \mathbf{n}_q as we are computing T_c for s -wave pairing. We therefore define $\bar{\delta D} = \int_0^{2\pi} \frac{d\theta}{2\pi} \delta D(\theta)$, where θ is the angle between \mathbf{n}_k and \mathbf{n}_q . Using that to first order in λ ,

$$\lambda \frac{T_c}{N_0} \sum_{|\Omega_m| < \omega_D} \int_0^\infty q dq \frac{1}{2\pi \Omega_m^2 + \varepsilon_q^2} = 1, \quad (3.22)$$

we obtain from (3.21)

$$\lambda \frac{T_c}{N_0} \sum_{|\Omega_m| < \omega_D} \int \frac{d^2 q}{(2\pi)^2} \frac{1}{\Omega_m^2 + \varepsilon_q^2} = 1 - \lambda \bar{\delta D} + O(\lambda^2). \quad (3.23)$$

We see that the KL renormalization of the interaction changes $1/\lambda$ to $1/\lambda - \delta\bar{D}$. For $E_F \gtrsim E_0$, $T_c \propto e^{-1/\lambda}$ then acquires a factor $e^{\delta\bar{D}}$. For $E_F \lesssim E_0$, $T_c \propto e^{-2/\lambda}$, and the factor is $e^{2\delta\bar{D}}$.

The calculation of $\delta\bar{D}$ is somewhat involved and is presented in Appendix A. The results are as follows: for $E_F \gg \omega_D$, $\delta\bar{D}$ is small in ω_D/E_F , in agreement with Migdal's theorem. At $E_0 \ll E_F \ll \omega_D$, we find $\delta\bar{D} = -3/2$, so the KL renormalization reduces T_c by $e^{3/2}$. At $E_F \ll E_0$, we find $\delta\bar{D} = 3/2$. Hence, the KL renormalization increases T_c by e^3 . In the last regime, $\mu_c < 0$ and we take $\delta D(\theta) = \delta D(0, 0; 0, 0)$ to be constant. As before, this is since we are keeping $O(\lambda)$ terms and neglecting terms of $O(\lambda^2)$.

The sign change of $\delta\bar{D}$ between $E_0 \ll E_F \ll \omega_D$ and $E_F \ll E_0$ is specific to 2D and can be understood by analytically computing δD at $T = 0$. The sign change occurs at $E_0 \sim E_F$, when μ_c changes sign. To see this, we note that each diagram for δD in Fig. 1 is the convolution of the interaction $V_0(\Omega_m)$ and two Green's functions. For $E_F \sim E_0 \ll \omega_D$, the relevant internal momenta and frequencies in the Green's functions are much larger than the relevant external ones. Therefore, up to an overall factor, each KL term is given by

$$J = \int_{-\infty}^{\infty} d\Omega_m \frac{\omega_D^2}{\Omega_m^2 + \omega_D^2} \int_{-\mu}^{\Lambda} \frac{d\varepsilon}{(i\Omega_m - \varepsilon_+)(i\Omega_m - \varepsilon_-)}, \quad (3.24)$$

where we have introduced a cutoff Λ , and ε_+ and ε_- are the energies for two nearly coinciding momenta. That is, the difference between relevant ε_+ and ε_- are on the order of $|\mu_c| \ll \omega_D$, while typical ε_+ and ε_- are on the order of ω_D .

The integral over Ω_m and ε in (3.24) is not singular and can be integrated in any order. Let us first integrate over Ω_m . Consider the case $\mu_c < 0$. Since $\varepsilon_+, \varepsilon_- > 0$ for negative μ_c , the frequency integral is entirely determined by the pole in the bosonic propagator at $\Omega_m = i\omega_D$. Once this pole is taken, we can safely set $\varepsilon_+ = \varepsilon_- = \varepsilon$ and integrate over dispersion. The integrand is singularity free, and we obtain

$$J_{\mu_c < 0} = \pi \frac{\omega_D}{\omega_D + |\mu_c|} \frac{\Lambda - |\mu_c|}{\Lambda + \omega_D}. \quad (3.25)$$

For positive μ_c there are two contributions to J : $J_{\mu_c > 0} = J_{1, \mu_c > 0} + J_{2, \mu_c > 0}$. The contribution ($J_{1, \mu_c > 0}$) again comes from the pole in the bosonic propagator. For this one can set, as before, $\varepsilon_+ = \varepsilon_- = \varepsilon$ and take the pole of $V_0(\Omega_m)$ in the frequency half-plane where there is no double pole in the fermionic propagator. Afterwards, one can integrate over ε . This procedure is again free from singularities, and the result is

$$J_{1, \mu_c > 0} = \pi \frac{\omega_D}{\omega_D + \mu_c} \frac{\Lambda + \mu_c}{\Lambda + \omega_D} + 2\pi \frac{\Lambda \mu_c}{(\omega_D + \mu_c)(\Lambda + \omega_D)}. \quad (3.26)$$

At $\mu_c = 0$, this term coincides with the one in Eq. (3.25).

The second contribution comes from the split poles in the fermionic propagators, from the range where ε_+ and ε_- have opposite signs. Because $|\mu_c|$ is much smaller than ω_D , the corresponding Ω_m are small compared to ω_D . The term $J_{2, \mu_c > 0}$ is then, up to an overall factor, the product of the static interaction [set equal to 1 in Eq. (3.24)] and the static particle-hole susceptibility. The latter is independent of μ_c (for

$\mu_c > 0$) in 2D and is equal to -2π . We hence have

$$J_{2, \mu_c > 0} = -2\pi. \quad (3.27)$$

Combining Eqs. (3.26) and (3.27), we find that near $\mu_c = 0$, $J_{\mu_c > 0}$ has an additional -2π compared to $J_{\mu_c < 0}$:

$$J_{\mu_c > 0} = \pi \frac{\omega_D}{\omega_D + \mu_c} \frac{\Lambda + \mu_c}{\Lambda + \omega_D} - 2\pi \frac{\omega_D(\Lambda + \omega_D + \mu_c)}{(\omega_D + \mu_c)(\Lambda + \omega_D)}. \quad (3.28)$$

Therefore, the KL contribution to the pairing vertex, and hence, to the prefactor of T_c , jumps by a finite value between $E_F \gtrsim E_0$, where $\mu_c > 0$ and $E_F \lesssim E_0$, where $\mu_c < 0$.

This discontinuity is in fact artificial, because we computed J at $T = 0$, when the static particle-hole susceptibility $\chi(\mu_c)$ is discontinuous at $\mu_c = 0$. At finite $T = T_c$, it is continuous, but varies rapidly in the range $|\mu_c| \leq T_c$. Accordingly, the KL correction to the exponent is continuous, but varies rapidly around $E_F \sim E_0$. We note in passing that the same discontinuity between $J_{\mu_c > 0}$ and $J_{\mu_c < 0}$ can be obtained if one approximates $V_0(\Omega_m)$ by a step function.

We also note that the magnitude of the KL renormalization for $\mu_c < 0$ depends on the ratio Λ/ω_D . For $\Lambda \gg \omega_D$, the magnitude of the KL correction is the same at positive and negative μ_c , only the sign is different: $J_{\mu_c < 0} \approx \pi$, $J_{\mu_c > 0} \approx -\pi$. For $\Lambda \ll \omega_D$, the KL renormalization at $\mu_c < 0$ becomes parametrically small: $J_{\mu_c < 0} \approx \pi \Lambda/\omega_D \ll 1$. This last result is consistent with earlier studies, which have found [7,43] that for a static interaction the KL renormalization vanishes for $\mu_c < 0$. To verify this, it is convenient to evaluate $J_{\mu_c < 0}$ by integrating over ε first. Doing so, one finds that typical frequencies are of order Λ . Hence, for $\Lambda \ll \omega_D$ the interaction term $\omega_D^2/(\omega_D^2 + \Omega_m^2)$ can be treated as static.

D. Total $O(\lambda)$ corrections to the exponent, and the renormalization of T_c

We now combine the renormalizations from self-energy, frequency dependence of the interaction, and KL renormalization. To first order in λ , the numerical prefactor for T_c is the product of the renormalizations from these three sources. Our analytical results for these prefactors are shown in Table II.

1. The case $E_F \gg \omega_D$

Here only self-energy and frequency dependence of the interaction affect the prefactor for T_c . The result is

$$T_c = 0.252\omega_D \exp(-1/\lambda). \quad (3.29)$$

This formula has been obtained earlier [2–6,8,49], and is presented here for completeness.

2. The case $E_0 \ll E_F \ll \omega_D$

In this regime we have

$$T_c = \frac{2e^\gamma}{\pi} e^{-1/4} e^{\delta\bar{D}} \sqrt{\omega_D E_F} \exp(-Z/\lambda) \quad (3.30)$$

$$= 0.12 \sqrt{\omega_D E_F} \exp(-1/\lambda). \quad (3.31)$$

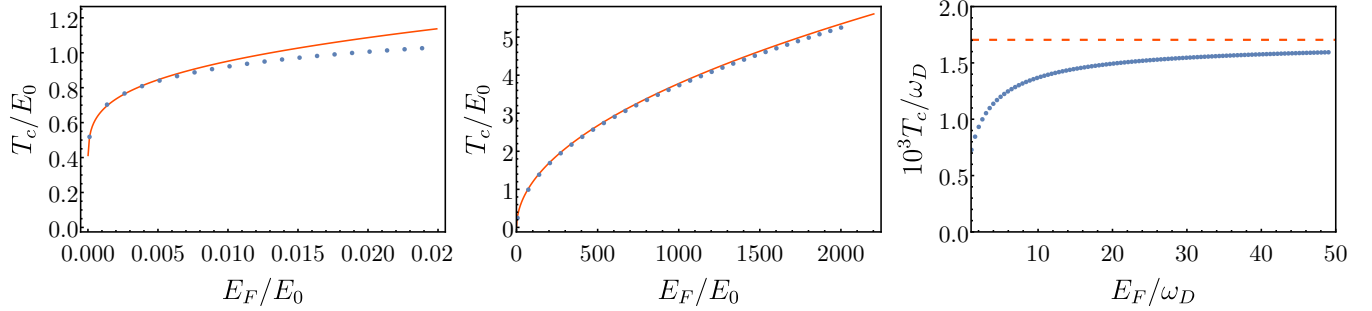


FIG. 5. T_c as a function of E_F in the three regimes $E_F \gg \omega_D$, $\omega_D \gg E_F \gg E_0$, and $E_0 \gg E_F$. The orange curves are our analytic expressions for T_c , derived in each region. At $E_F \ll E_0$ we included into the analytical expression the leading corrections to T_c of order $O[\log \log(E_0/E_F)/\log(E_0/E_F)]$. Our numerical results for T_c were found by self-consistently solving for T_c and μ_c as a function of E_F . We used $\lambda = 0.2$, whereby $E_0 \approx 0.45 \times 10^{-4} \omega_D$. The limiting value of T_c at large E_F/ω_D is $T_c = 0.252 \omega_D e^{-1/\lambda} \approx 1.7 \times 10^{-3} \omega_D$ (the dashed line in the last panel).

3. The case $E_F \ll E_0$

In this regime we have $T_c = |\mu_c|/\log(|\mu_c|/E_F)$ and

$$|\mu_c| = e^{2\bar{\delta}D} e^{-1/2} \omega_D \exp(-2Z/\lambda) = e^{3/2} E_0 \approx 4.48 E_0. \quad (3.32)$$

Hence, to leading order in $\log E_0/E_F$, we obtain

$$T_c = 4.48 \frac{E_0}{\log(E_0/E_F)}. \quad (3.33)$$

IV. NUMERICAL CALCULATION OF T_c

For general values of E_F , we calculate T_c numerically by simultaneously solving Eqs. (2.5) and (3.23). In Fig. 5 we present the numerical results for T_c in the three regions of E_F ($E_F \gg \omega_D$, $\omega_D \gg E_F \gg E_0$, and $E_0 \gg E_F$) and compare them with our analytic expressions. We see good agreement between analytical and numerical results for all values of E_F . This figure summarizes the key results of our work.

In Fig. 6 we present the result of our numerical evaluations of the KL correction $\bar{\delta}D$ over a wide range of E_F , obtained by using the numerically obtained $\mu_c(E_F)$ and $T_c(E_F)$. We see from Fig. 6 that the KL correction is small for $E_F \gg \omega_D$, in agreement with Migdal's theorem. As E_F is decreased, $\bar{\delta}D$ reaches a sizable finite value close to -1.5 at $E_F \sim 10^3 E_0 \sim 0.1 \omega_D$. Upon further reduction of the particle density, we cross the region where $E_F \sim E_0$. Here $\bar{\delta}D$ changes sign, and saturates at 1.5 for smaller E_F/E_0 . This limiting behavior agrees well with our analytical results.

The shaded region in Fig. 6 marks the range near $E_F \sim E_0$, where the result for $\bar{\delta}D$ is more subtle and depends on whether the calculations are done perturbatively or self-consistently. This also affects the behavior of T_c and μ_c as functions of E_F/E_0 . In the perturbative calculation, one computes $\bar{\delta}D$ by using “bare” values of μ_c and T_c , obtained without $O(\lambda)$ corrections. The bare $\mu_c(E_F)$ is obtained by solving Eqs. (2.4) and (2.5), and is a continuous function of E_F/E_0 . Additionally, one can show that the bare μ_c changes sign at $E_F = \frac{2}{\pi} \log(2) e^\gamma E_0 \approx 0.8 E_0$.

Accordingly, $\bar{\delta}D$, computed using the bare $\mu_c(E_F)$ and $T_c(E_F)$, is also a continuous function of E_F and also changes sign at $E_F \approx 0.8 E_0$. We show this perturbative result for $\bar{\delta}D$ in Fig. 7(c). Combining this perturbative $\lambda \bar{\delta}D$ with other $O(\lambda)$ corrections, we obtain the result for the renormalized μ_c and

T_c , which we present in Figs. 7(a) and 7(e). We see that while T_c is a continuous function of E_F/E_0 , it is not monotonic, having a maximum at $E_F \sim 0.04 E_0$.

The problem with the above perturbative calculation is that the bare μ_c and T_c are used to compute $\bar{\delta}D$, which is highly sensitive to where (at which E_F/E_0) μ_c changes sign, as well as how μ_c evolves with E_F/E_0 . Meanwhile, $O(\lambda)$ corrections, although nominally small, add factors $O(1)$ to both T_c and μ_c . This is since both T_c and μ_c go as $\exp(-2/\lambda)$ for $E_F \lesssim E_0$, and $O(\lambda)$ corrections to the exponent change both by $O(1)$.

Therefore the value of E_F/E_0 at which μ_c changes sign, also changes by $O(1)$. One can see this in Fig. 7(a), where the “dressed” μ_c calculated perturbatively changes sign at $E_F \approx 0.4 E_0$, rather than $E_F \approx 0.8 E_0$ as it did originally. This significantly affects the behavior of $\bar{\delta}D$, which in turn leads to $O(1)$ corrections to μ_c and T_c . This mutual dependence clearly calls for a fully self-consistent calculation of T_c in the

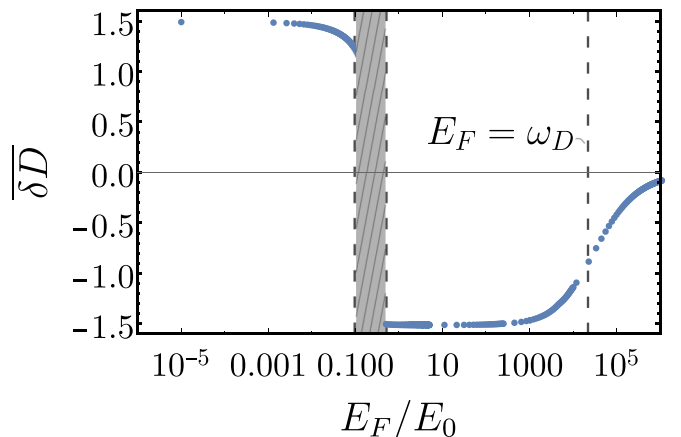


FIG. 6. The result of the numerical evaluation of the KL correction to s -wave pairing interaction $\bar{\delta}D$ as a function of E_F/E_0 for a wide range of E_F . The KL correction is small at $E_F \gg \omega_D$, in agreement with Migdal's theorem, but becomes sizable at smaller E_F and evolves from $\bar{\delta}D \approx -1.5$ to $\bar{\delta}D \approx 1.5$ at $E_F \sim 0.17 E_0$. The behavior near $E_F \sim 0.17 E_0$ (the shaded region in the figure) requires more detailed consideration. We show the behavior in this region in Fig. 7.

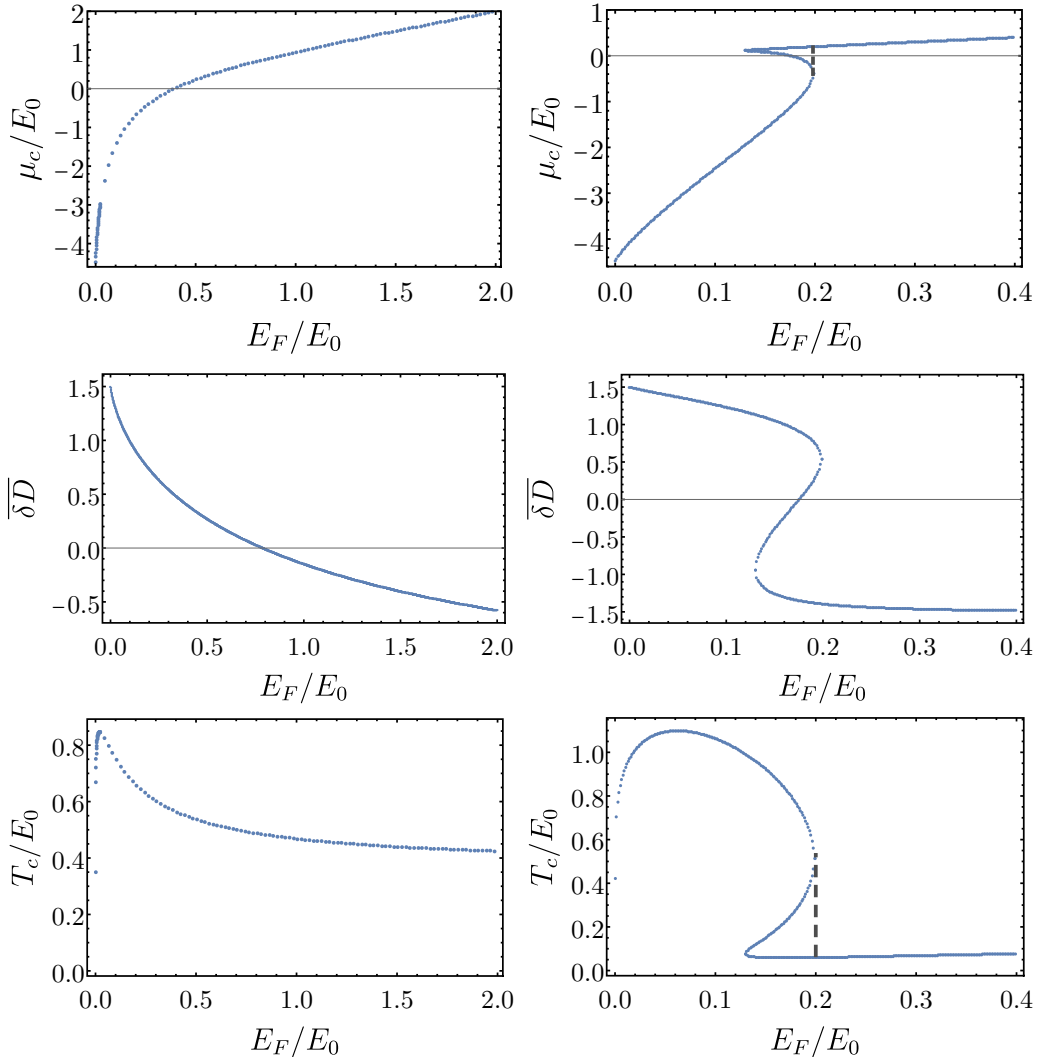


FIG. 7. The numerically calculated values of T_c , μ_c , and $\overline{\delta D}$ in the region where the KL correction changes sign. The plots on the left are calculated within strict perturbation theory, while the plots on the right are calculated self-consistently. Self-consistent calculations yield multivalued quantities around $E_F \approx 0.2E_0$, which in practice means that T_c and μ_c change discontinuously upon variation of E_F/E_0 (dashed lines on the right-hand-side panels for T_c and μ_c).

range $E_F \sim E_0$, where $\overline{\delta D}$ rapidly evolves. In other ranges of E_F/E_0 , where $\overline{\delta D}$ saturates and only weakly varies with E_F/E_0 , self-consistency is not required.

We show the results of self-consistent calculations of μ_c , $\overline{\delta D}$, and T_c in the right three panels of Fig. 7. To obtain these results, we treat $\overline{\delta D}$ as a function of T_c and μ_c , and substitute $\overline{\delta D}(\mu_c, T_c)$ into Eq. (3.23). This equation is then solved self-consistently with Eq. (2.5). We see from the plots that over some range of E_F/E_0 , T_c is a multivalued function of E_F/E_0 . In practical terms this implies that the superconducting transition temperature (the largest possible T_c for a given E_F/E_0) jumps by a finite amount at $E_F \sim 0.2E_0$. There is of course a corresponding jump in μ_c at this E_F/E_0 . Though subleading corrections to T_c may yield a continuous transition, T_c should change sharply around $E_F/E_0 = 0.2$ in either case. Note that the maximum in T_c at smaller values of E_F also emerges in a self-consistent calculation, but is located at a larger $E_F \approx 0.06E_0$.

V. CONCLUSION

In this paper we derived expressions for the onset temperature of the pairing (T_c in Eliashberg approximation) with exact prefactors for quasi-2D electrons, with Einstein-phonon-mediated attraction at weak coupling. Previous studies chiefly considered the adiabatic limit $E_F \gg \omega_D$. We analyzed T_c in the two other regimes $E_F \ll E_0$ and $\omega_D \gg E_F \gg E_0$, where $E_0 = \omega_D e^{-2/\lambda}$ is the bound state energy for two fermions in a vacuum and λ is the dimensionless electron-phonon coupling constant. In these two regimes the corrections to T_c come from three sources: fermionic self-energy, frequency dependence of the phonon-mediated interaction, and KL renormalization of the pairing interaction by particle-hole excitations. KL corrections are small in ω_D/E_F in the adiabatic regime, but become $O(1)$ in the other two regimes. We found that the combined renormalization from the three sources reduces T_c from its mean-field value by a factor of almost 10 in the intermediate regime $E_0 \ll E_F \ll \omega_D$, and increases T_c by

nearly a factor of 5 in the regime $E_F \ll E_0$, which corresponds to very low carrier concentration. We hope that our results will form a starting point for studies of T_c beyond logarithmical accuracy in the physically more relevant case when both electron-electron repulsion and electron-phonon attraction are present.

ACKNOWLEDGMENTS

We are thankful to M. Christensen, R. Fernandes, M. Gastiasoro, A. Klein, A. Millis, N. Prokofiev, and B. Svistunov for useful discussions. This work was funded by the Department of Energy through the University of Minnesota Center for Quantum Materials, under DE-SC-0016371.

APPENDIX A: EVALUATION OF THE KL CORRECTIONS

Here we calculate the KL corrections $\delta D(k, q)$ to the interaction. This is a sum of two types of diagrams: vertex corrections and exchange corrections, and we will write $\delta D = D_1^{\text{vertex}} + D_2^{\text{vertex}} + D^X$. Before calculating these diagrams, we discuss the relevant values of these parameters in the various limits for E_F .

As discussed in Sec. III C, we will calculate δD at zero external frequency, and with the magnitudes of \mathbf{k} and \mathbf{q} fixed to $\Theta(\mu_c)k_\mu$. Depending on the value of E_F , there are

essentially three limiting regions:

(A) $\mu_c < 0$ and $|\mu_c| \gg T_c$: This is where $E_F \ll E_0$.

(B) $\mu_c \approx 0$ and $T_c \gg |\mu_c|$: This region describes the crossover between $E_F \ll E_0$ and $E_0 \ll E_F \ll \omega_D$.

(C) $\mu_c > 0$ and $\mu_c \gg T_c$: This includes the regions $E_0 \ll E_F \ll \omega_D$ and $E_F \gg \omega_D$.

In both regions A and C we have $|\mu_c| \gg T_c$. Since T_c is therefore smallest energy scale in the calculation, we may simply evaluate these diagrams at $T = 0$ as an approximation. We also fix the external frequencies equal to zero in both regions A and C.

Regarding region B where $\mu_c \approx 0$, we cannot evaluate these diagrams at $T = 0$, since T_c is not the smallest energy scale in the problem. However, we will still calculate these diagrams at zero external frequency and momenta. The validity of setting the external frequency and momenta to zero will be discussed below.

1. Vertex corrections

Let us first consider the vertex corrections, denoted D_1^{vertex} and D_2^{vertex} . One can verify that these two corrections will end up being equal, so we will calculate D_1^{vertex} and take $D^{\text{vertex}} = 2D_1^{\text{vertex}}$. Referring to Fig. 1, we write the expression for D^{vertex} below, where we have used $D_0(\omega_m) = \omega_D^2/(\omega_m^2 + \omega_D^2)$, $G(k) = (i\omega_m - \varepsilon_k)^{-1}$, and $\varepsilon_k = k^2/2m - \mu_c$:

$$\lambda D^{\text{vertex}} = 2gT_c D_0(\omega_p) \sum_{\Omega_m} \int \frac{d^2l}{(2\pi)^2} \frac{1}{i\Omega_m + i\omega_q - \varepsilon_l} \frac{1}{i\Omega_m + i\omega_q + i\omega_p - \varepsilon_{l+p}} D_0(\Omega_m). \quad (\text{A1})$$

In the above expression we have defined $\mathbf{p} = \mathbf{k} - \mathbf{q}$ and $\omega_p = \omega_k - \omega_q$, and Ω_m is a bosonic Matsubara frequency. Since $\omega_p = \omega_k - \omega_q$ is on the order of $T_c \ll \omega_D$, we may replace $D_0(\omega_p) = 1$. Using partial fractions we find

$$\lambda D^{\text{vertex}} = 2gT_c \sum_{\Omega_m} \int \frac{d^2l}{(2\pi)^2} \frac{1}{\varepsilon_{l+p} - \varepsilon_l - i\omega_p} \left(\frac{1}{i\Omega_m + i\omega_q + i\omega_p - \varepsilon_{l+p}} - \frac{1}{i\Omega_m + i\omega_q - \varepsilon_l} \right) D_0(\Omega_m). \quad (\text{A2})$$

Calculating the Matsubara sum, and setting $n_B(\omega_D) = 0$ (since $T_c \ll \omega_D$), we have

$$\lambda D^{\text{vertex}} = g\omega_D \int \frac{d^2l}{(2\pi)^2} \frac{1}{\varepsilon_{l+p} - \varepsilon_l - i\omega_p} \left(\frac{n_F(\varepsilon_{l+p})}{i\omega_q + i\omega_p - \varepsilon_{l+p} + \omega_D} - \frac{1 - n_F(\varepsilon_{l+p})}{\omega_D + \varepsilon_{l+p} - i\omega_q - i\omega_p} \right. \\ \left. - \frac{n_F(\varepsilon_l)}{i\omega_q - \varepsilon_l + \omega_D} + \frac{1 - n_F(\varepsilon_l)}{\omega_D + \varepsilon_l - i\omega_q} \right). \quad (\text{A3})$$

Now we may simplify our three different limits.

a. Region A

Let us begin with region A, where $|\mu_c| \gg T_c$ and $\mu_c < 0$. All Fermi functions are effectively zero in this region, and we have after some algebra

$$\lambda D_A^{\text{vertex}} = g\omega_D \int \frac{d^2l}{(2\pi)^2} \frac{1}{\omega_D + \varepsilon_l - i\omega_q} \frac{1}{\omega_D + \varepsilon_{l+p} - i\omega_q - i\omega_p}. \quad (\text{A4})$$

As discussed above, in region A, we set all external frequencies and momenta to zero. This expression then becomes

$$\lambda D_A^{\text{vertex}} = gN_0\omega_D \int_{-\mu_c}^{\infty} d\varepsilon \frac{1}{(\omega_D + \varepsilon)^2} \quad (\text{A5})$$

$$= \lambda \frac{\omega_D}{\omega_D - \mu_c}. \quad (\text{A6})$$

Since $\mu_c \ll \omega_D$ in region A, we have $D_A^{\text{vertex}} \approx 1$. As alluded to in the main text, this KL correction is nonzero in region A (where $\mu_c < 0$). From this calculation, we see that

this is due to the dynamical nature of our interaction (more precisely, the presence of a pole in our bosonic propagator).

b. Region B

In this region we must now include the terms with Fermi functions. For reasons that will become clear below, we will refer to this as the singular part of D^{vertex} . Regarding the terms without Fermi functions, we may simply take our above result from region A, since we are still working at zero external momenta and frequencies. We will refer to this expression as the regular part of D^{vertex} . Focusing on the singular part of D^{vertex} , we have

$$\lambda D_{\text{sing}}^{\text{vertex}} = g\omega_D \int \frac{d^2l}{(2\pi)^2} \frac{1}{\varepsilon_{l+p} - \varepsilon_l - i\omega_p} \times \left(\frac{n_F(\varepsilon_{l+p})}{i\omega_q + i\omega_p - \varepsilon_{l+p} + \omega_D} + \frac{n_F(\varepsilon_{l+p})}{\omega_D + \varepsilon_{l+p} - i\omega_q - i\omega_p} - \frac{n_F(\varepsilon_l)}{i\omega_q - \varepsilon_l + \omega_D} - \frac{n_F(\varepsilon_l)}{\omega_D + \varepsilon_l - i\omega_q} \right). \quad (\text{A7})$$

Since ω_D is the largest energy scale in region B, we simply replace the denominators of all Fermi functions by ω_D , obtaining

$$\lambda D_{\text{sing}}^{\text{vertex}} \approx 2g \int \frac{d^2l}{(2\pi)^2} \frac{n_F(\varepsilon_{l+p}) - n_F(\varepsilon_l)}{\varepsilon_{l+p} - \varepsilon_l - i\omega_p}. \quad (\text{A8})$$

Working in the static limit, and taking $p \rightarrow 0$, we find

$$\lambda D_{\text{sing}}^{\text{vertex}}(p=0) = 2g \int \frac{d^2l}{(2\pi)^2} \frac{dn_F(\varepsilon_l)}{d\varepsilon_l} \quad (\text{A9})$$

$$= 2gN_0 \int_{-\mu_c}^{\infty} d\varepsilon \frac{dn_F(\varepsilon)}{d\varepsilon} \quad (\text{A10})$$

$$= -2\lambda n_F(-\mu_c), \quad (\text{A11})$$

so we have $D_{\text{sing}}^{\text{vertex}}(p=0) = -2n_F(-\mu_c)$. Note that this Fermi function leads to a steplike jump as we transition from region A to region C through region B. This is why we refer to it as singular. In contrast, the other part of this vertex correction is essentially 1 across the transition, which is why we called it the regular part of D^{vertex} . Putting $D_{\text{reg}}^{\text{vertex}}$ and $D_{\text{sing}}^{\text{vertex}}$ together, we find $D_B^{\text{vertex}}(p=0) = -\tanh \frac{\mu_c}{2T_c}$.

c. Region C

As in region A we have $|\mu_c| \gg T_c$ and we can again evaluate this expression at $T = 0$. However, both the regular and singular pieces of the vertex correction now contribute since $\mu_c > 0$ (we cannot set the Fermi functions to zero). However, we can use our $T = 0$ approximation to replace the Fermi function $n_F(x)$ with $\Theta(-x)$. Using this and $1 - \Theta(-x) = \Theta(x)$, we find

$$\lambda D_C^{\text{vertex}} = g\omega_D P \int \frac{d^2l}{(2\pi)^2} \frac{1}{\varepsilon_{l+p} - \varepsilon_l} \left(\frac{\Theta(-\varepsilon_{l+p})}{-\varepsilon_{l+p} + \omega_D} - \frac{\Theta(\varepsilon_{l+p})}{\omega_D + \varepsilon_{l+p}} - \frac{\Theta(-\varepsilon_l)}{-\varepsilon_l + \omega_D} + \frac{\Theta(\varepsilon_l)}{\omega_D + \varepsilon_l} \right). \quad (\text{A17})$$

We rewrite the step functions in terms of sgn functions, obtaining

$$\lambda D_C^{\text{vertex}} = g\omega_D P \int \frac{1}{\varepsilon_{l+p} - \varepsilon_l} \left(-\frac{\text{sgn}(\varepsilon_{l+p})}{\omega_D + |\varepsilon_{l+p}|} + \frac{\text{sgn}(\varepsilon_l)}{\omega_D + |\varepsilon_l|} \right) \quad (\text{A18})$$

$$= 2g\omega_D P \int \frac{ldl}{2\pi} \frac{\text{sgn}(\varepsilon_l)}{\omega_D + |\varepsilon_l|} \int \frac{d\theta}{2\pi} \frac{1}{p^2/2m + lp \cos(\theta)/m}. \quad (\text{A19})$$

This is what we use in the numerical calculations of T_c . As we will see below, this expression which was evaluated at $p = 0$ overestimates the effect of the singular piece in the crossover region. However, it has the correct qualitative behavior, i.e., the vertex corrections smoothly decrease from 1 to -1 connecting the limiting behaviors of both region A and region C.

With this, we now turn to the complications discussed above that we cannot naively evaluate this diagram at $p = \omega_p = 0$. Instead we must consider momenta q and k such that ε_q and ε_k are on the order of T_c . We will see that in this crossover region where $|\mu_c| \ll T_c$, the $D_{\text{sing}}^{\text{vertex}}(p)$ dies quickly with increasing p . This invalidates the assumption made in the main text, that the KL diagram is relatively constant over the region of \mathbf{q} which contribute significantly to the integral. In fact, the quick decay of $D_{\text{sing}}^{\text{vertex}}(p)$ with p destroys the logarithmical singularity in the second term of Eq. (3.21). Therefore, the effect on T_c in region B due to the vertex correction is not due to the singular piece, but the regular piece.

To show this, let us rewrite $D_{\text{sing}}^{\text{vertex}}(p)$ and take $\mu_c = 0$ for convenience. Using Eq. (A8) we have

$$\lambda D_{\text{sing}}^{\text{vertex}}(p) = 2g \int \frac{d^2l}{(2\pi)^2} \frac{n_F(\varepsilon_{l+p}) - n_F(\varepsilon_l)}{\varepsilon_{l+p} - \varepsilon_l - i\omega_p} \quad (\text{A12})$$

$$= 2g \int \frac{d^2l}{(2\pi)^2} \left(\frac{n_F(\varepsilon_l)}{\varepsilon_l - \varepsilon_{l+p} - i\omega_p} - \frac{n_F(\varepsilon_l)}{\varepsilon_{l+p} - \varepsilon_l - i\omega_p} \right) \quad (\text{A13})$$

$$= -2gP \int \frac{d^2l}{(2\pi)^2} \frac{n_F(\varepsilon_l)}{\varepsilon_{l+p} - \varepsilon_l}. \quad (\text{A14})$$

To obtain the last equality, we took $\omega_p = 0$ for simplicity. Doing the angular integration, we find

$$D_{\text{sing}}^{\text{vertex}}(p) = -\frac{2}{p} \int_0^{p/2} \frac{dl n_F(\varepsilon_l)}{\sqrt{(p/2)^2 - l^2}} \quad (\text{A15})$$

$$\approx -2n_F[\varepsilon(p/2)]. \quad (\text{A16})$$

To obtain the final expression, we first notice that the integrand peaks when $l = p/2$. Therefore, as a crude approximation, we pull $n_F(\varepsilon_l)$ outside of the integral, evaluated at $l = p/2$, and do the remaining integral. As asserted above, this expression decays quickly with p . One may verify that this indeed leads to the disappearance of the logarithmical singularity upon insertion into Eq. (3.21).

Doing the angular integration and canceling a factor of $\lambda = gN_0$, we find

$$D_C^{\text{vertex}} = \frac{2\omega_D}{p} \int_0^{p/2} \frac{l dl}{\sqrt{(p/2)^2 - l^2}} \frac{\text{sgn}(\varepsilon_l)}{\omega_D + |\varepsilon_l|}. \quad (\text{A20})$$

Since in region C we set the external momenta q and k equal to k_μ , we have $p = |\mathbf{q} - \mathbf{k}| = 2k_\mu \sin \theta/2$, where θ is the angle between \mathbf{q} and \mathbf{k} . Therefore, the upper limit of this integral is $p/2 = k_\mu \sin \theta/2 < k_\mu$. Since $\varepsilon_l = l^2/2m - \mu_c$, if $l < k_\mu$ (as in the above integral), we have $\varepsilon_l < 0$. Therefore, we set $\text{sgn}(\varepsilon_l) = -1$ and $|\varepsilon_l| = \mu_c - l^2/2m$, obtaining

$$D_C^{\text{vertex}} = -\frac{2\omega_D}{p} \int_0^{p/2} \frac{l dl}{\sqrt{(p/2)^2 - l^2}} \frac{1}{\omega_D + \mu_c - l^2/2m}. \quad (\text{A21})$$

We now rescale $l = k_\mu x$ and $\bar{\mu}_c = \mu_c/\omega_D$, plug in $p = 2k_\mu \sin \theta/2$, and average over all θ to obtain

$$\overline{D_C^{\text{vertex}}(\bar{\mu}_c)} = -\frac{1}{\pi} \int_0^\pi d\theta \frac{1}{\sin(\theta/2)} \int_0^{\sin(\theta/2)} \frac{x dx}{\sqrt{\sin^2(\theta/2) - x^2}} \frac{1}{1 + \bar{\mu}_c(1 - x^2)}. \quad (\text{A22})$$

This is the expression we use to numerically calculate the vertex corrections for any μ_c in region C. We can simplify this expression analytically in the limit of large and intermediate density ($E_F \gg \omega_D$ and $\omega_D \gg E_F \gg E_0$), obtaining $\overline{D_C^{\text{vertex}}} = 0$ and $\overline{D_C^{\text{vertex}}} = -1$, respectively. Note that the vertex corrections go to zero in the limit of small ω_D/E_F in accordance with Migdal's theorem.

2. Exchange diagram

We now move on to the exchange diagram, which we will denote D^X . We have from Fig. 1

$$\lambda D^X = gT \sum_{\Omega_m} \int \frac{d^2 l}{(2\pi)^2} G_0(l) G_0(l+p) D_0(\Omega_m - \omega_q) D_0(\Omega_m - \omega_k), \quad (\text{A23})$$

where we have redefined $\omega_p = -(\omega_q + \omega_k)$, $\mathbf{p} = -(\mathbf{q} + \mathbf{k})$, and Ω_m is a fermionic Matsubara frequency. If we let $\Omega_m \rightarrow \Omega_m - \omega_q$, we have instead

$$\lambda D^X = gT \sum_{\Omega_m} \int \frac{d^2 l}{(2\pi)^2} \frac{1}{i\Omega_m + i\omega_q - \varepsilon_l} \frac{1}{i\Omega_m + i\omega_q + i\omega_p - \varepsilon_{l+p}} D_0(\Omega_m) D_0(\Omega_m + \omega_q - \omega_k), \quad (\text{A24})$$

where the redefined Ω_m is now bosonic. Since ω_k and ω_q are on the order of $T \ll \omega_D$, we may approximate this sum with

$$\lambda D^X = gT \sum_{\Omega_m} \int \frac{d^2 l}{(2\pi)^2} \frac{1}{i\Omega_m + i\omega_q - \varepsilon_l} \frac{1}{i\Omega_m + i\omega_q + i\omega_p - \varepsilon_{l+p}} D_0(\Omega_m)^2. \quad (\text{A25})$$

Note that the expressions for D^{vertex} and D^X are identical except for a difference of 2 in the prefactor and the fact that $D_0(\Omega_m)$ is squared in the exchange diagram. We will exploit this similarity to obtain expressions for D^X in all three regions from our previous work. Using the definition of $D_0(\Omega_m)$, one may verify

$$\frac{d}{d\omega_D^2} \frac{D_0(\Omega_m)}{\omega_D^2} = -\frac{D_0(\Omega_m)^2}{\omega_D^4}. \quad (\text{A26})$$

We therefore have

$$D^X(p, \omega_p) = -\frac{\omega_D^4}{2} \frac{d}{d\omega_D^2} \left(\frac{1}{\omega_D^2} D^{\text{vertex}}(p, \omega_p) \right). \quad (\text{A27})$$

We have explicitly written the dependence on ω_p and p to emphasize that this identity is true only before we write how p depends on k and q . This is because in the case of the vertex corrections above, $p = k - q$, while for the exchange corrections, $p = -q - k$. We now use this derivative formula to calculate D^X in our three limits.

a. Region A

In region A we have $p = -q - k = 0$. Applying our derivative formula [Eq. (A27)] to our previous result in region A, $D^{\text{vertex}} = 1/(1 - \bar{\mu}_c)$, we obtain

$$D_A^X = \frac{1}{4} \frac{2 - \bar{\mu}_c}{(1 - \bar{\mu}_c)^2} \approx \frac{1}{2}. \quad (\text{A28})$$

b. Region B

In region B we also have $p = 0$. Applying our derivative formula to our previous equation in region B, we obtain

$$D_B^X = -\frac{1}{2} \tanh \frac{\mu_c}{2T_c}. \quad (\text{A29})$$

As before, this is a sum of regular and singular parts, with the singular piece switching on across $\mu_c = 0$. As before, this expression overestimates the effect of the singular piece, which does not affect T_c until $|\mu_c|$ exceeds T_c .

TABLE III. The summary of the analytic results of this paper regarding the KL corrections. These directly affect the prefactor of T_c in each region for E_F .

	$\overline{D^{\text{vertex}}}$	$\overline{D^{\text{exchange}}}$	$\overline{\delta D}$
$E_F \ll E_0$	1	1/2	3/2
$E_0 \ll E_F \ll \omega_D$	-1	-1/2	-3/2
$\omega_D \ll E_F$	0	0	0

c. Region C

Applying the derivative formula to Eq. (A20), we find

$$D_C^X(k, q) = \frac{1}{2p} \int_0^{p/2} dl \frac{\text{sgn } \varepsilon_l}{\sqrt{(p/2)^2 - l^2}} \frac{2 + |\bar{\varepsilon}_l|}{(1 + |\bar{\varepsilon}_l|)^2}, \quad (\text{A30})$$

where we have defined $\bar{\varepsilon}_l = \varepsilon_l/\omega_D$. Since we have $k = q = k_\mu$ in region C, we have $p = |\mathbf{k} + \mathbf{q}| = 2k_\mu \cos \theta/2$. We can now simplify this expression as before to obtain

$$\begin{aligned} \overline{D_C^X(\bar{\mu}_c)} &= -\frac{1}{4\pi} \int_0^\pi \frac{d\theta}{\cos(\theta/2)} \int_0^{\cos(\theta/2)} dx \frac{x}{\sqrt{\cos^2(\theta/2) - x^2}} \\ &\times \frac{2 + \bar{\mu}_c(1 - x^2)}{[1 + \bar{\mu}_c(1 - x^2)]^2}. \end{aligned} \quad (\text{A31})$$

This is the expression we use to numerically calculate the exchange contribution for any $\bar{\mu}_c$ in region C. As before, we can simplify this expression analytically when $\mu_c \ll \omega_D$ (corresponding to $E_0 \ll E_F \ll \omega_D$) and $\mu_c \gg \omega_D$ (corresponding to $E_F \gg \omega_D$), obtaining $-1/2$ and 0 , respectively.

d. Total KL contribution

The total correction to the interaction δD is found by summing the contribution from the vertex corrections and the exchange diagram $\delta D = D^{\text{vertex}} + D^{\text{exchange}}$. We can now numerically calculate KL contribution at any μ_c , given the region (A, B, or C) in which μ_c exists. Additionally, though we do not have an analytic expression that holds for general μ_c , we have obtained simple results for this correction in our general limits of E_F , which are summarized in Table III. The total correction as a function of E_F/E_0 as been plotted in Fig. 6.

APPENDIX B: DETAILS OF NUMERICAL CALCULATIONS

For our numerical calculation of T_c , we start from the full equation for the pairing vertex, Eq. (3.3), which we rewrite below for convenience:

$$\begin{aligned} \Phi(\omega_m, \mathbf{k}) &= -T \sum_{\Omega_m} \int \frac{d^2 q}{(2\pi)^2} G(\Omega_m, q) G(-\Omega_m, -q) \\ &\times V_{\text{eff}}(\omega_m, \mathbf{k}; \Omega_m, \mathbf{q}) \Phi(\Omega_m, \mathbf{q}). \end{aligned} \quad (\text{B1})$$

In the main text we discussed all three effects on T_c separately, and added their contributions at the end, which is valid at weak coupling. Doing so, our expression for the

pairing vertex becomes

$$\frac{T_c}{N_0} \sum_{\Omega_m} \int \frac{d^2 q}{(2\pi)^2} \frac{1}{Z^2 \Omega_m^2 + \varepsilon_q^2} \frac{\omega_D^4}{(\omega_D^2 + \Omega_m^2)^2} = \frac{Z}{\lambda} - \overline{\delta D}. \quad (\text{B2})$$

Integrating over momentum and doing one of the frequency sums, this equation becomes

$$\begin{aligned} \frac{1}{2} \log \left(\frac{2e^\gamma}{\sqrt{\varepsilon\pi} \bar{T}_c} \right) + \bar{T}_c \sum_{\Omega_m} \arctan \left(\frac{\bar{\mu}_c}{\Omega_m} \right) \frac{1}{(1 + \Omega_m^2)^2} \frac{1}{|\bar{\Omega}_m|} \\ = \frac{Z(\bar{\mu}_c)}{\lambda} - \overline{\delta D}(\bar{\mu}_c), \end{aligned} \quad (\text{B3})$$

where we have redefined all variables to be relative to ω_D , and emphasized the fact that Z and $\overline{\delta D}$ are functions of $\bar{\mu}_c$. We now rewrite the second term on the left-hand side as follows:

$$\begin{aligned} \bar{T}_c \sum_{\Omega_m} \arctan \left(\frac{\bar{\mu}_c}{\Omega_m} \right) \frac{1}{(1 + \Omega_m^2)^2} \frac{1}{|\bar{\Omega}_m|} \\ = \int_0^{\bar{\mu}_c} dx \left(\frac{-1}{x^2 - 1} \frac{1}{8\bar{T}_c} \text{sech}^2 \frac{1}{2\bar{T}_c} + \frac{x^2 - 3}{4(x^2 - 1)^2} \tanh \frac{1}{2\bar{T}_c} \right. \\ \left. + \frac{1}{2x(x^2 - 1)^2} \tanh \frac{x}{2\bar{T}_c} \right). \end{aligned} \quad (\text{B4})$$

This integral is more convenient than the original sum for computational purposes. To derive this expression, recall that for any function $f(\bar{\mu}_c)$, $f(\bar{\mu}_c) = \int_0^{\bar{\mu}_c} \frac{df(x)}{dx} dx$, assuming $f(0) = 0$. This is what we did above, where after taking the derivative, the sum has been evaluated explicitly. This simplified version of the equation for the pairing vertex is then solved simultaneously with $\bar{\mu}_c = \bar{T}_c \log[\exp(\bar{E}_F/\bar{T}_c) - 1]$ for a given E_F .

Though this can in principle be done for any E_F , we only use the above equation for $E_F > 5E_0$, and instead solve a simplified equation for $E_F < 5E_0$, where $|\mu_c| \ll \omega_D$. For $E_F > 5E_0$ we also use the Kohn-Luttinger expression calculated in region C, from the above Appendix. The threshold of $E_F = 5E_0$ is of course artificial. We only require $|\mu_c| \ll \omega_D$ for our simplified equation to apply, and we find that at $E_F = 5E_0$, $\mu_c/\omega_D = 2 \times 10^{-4} \ll 1$ (using $\lambda = 0.2$).

In the region where $|\mu_c| \ll \omega_D$, the above sum can be simplified to

$$\bar{T}_c \sum_{\bar{\Omega}_m} \arctan \left(\frac{\bar{\mu}_c}{\bar{\Omega}_m} \right) \frac{1}{\bar{\Omega}_m} = \int_0^{\bar{\mu}_c} dx \frac{1}{2x} \tanh \frac{x}{2\bar{T}_c}. \quad (\text{B5})$$

Additionally, for $|\mu_c| \ll \omega_D$, we may set $Z = 1 + \lambda/2$. The resulting equation for T_c can be written as

$$\log \left(\frac{2e^{\gamma-3/2}}{\pi \tilde{T}_c} \right) - 3 \tanh \frac{\tilde{\mu}_c}{2\tilde{T}_c} + \int_0^{\tilde{\mu}_c} \frac{\tanh \frac{x}{2\tilde{T}_c}}{x} = 0, \quad (\text{B6})$$

where all quantities with tildes have been expressed in terms of E_0 . Note that we have used the expression for the Kohn-Luttinger correction which applies only in the crossover region (region B), where $\mu_c \ll T_c$. It is in fact unnecessary to use the expression calculated in region A ($E_F \ll E_0$), since the expression in region B smoothly saturates to the constant value calculated in region A. This is the computationally more convenient equation we solve (both self-consistently and non-self-consistently), along with the equation for the chemical

potential for T_c and μ_c for $E_F \leq 5E_0$. All numerical results are obtained using $\lambda = 0.2$.

APPENDIX C: ASSUMPTION OF BANDWIDTH

Throughout this paper we have worked in the infinite bandwidth limit, i.e., the bandwidth Λ is much larger than E_F and ω_D . In general, the effect of the Kohn-Luttinger corrections will depend on the ratio Λ/ω_D . To illustrate this point, we will evaluate the vertex correction D^{vertex} at finite bandwidth. For simplicity, we will evaluate this correction at $\mu_c < 0$, for $|\mu_c| \gg T_c$ (see region A). Referring to our calculations in Appendix A, we may simply take Eq. (A6) and replace the

upper limit by Λ . The new result at finite bandwidth is then

$$D_A^{\text{vertex}} = \frac{\omega_D}{\omega_D - \mu_c} - \frac{\omega_D}{\omega_D - \Lambda}. \quad (\text{C1})$$

If we work in the limit where $|\mu_c| \ll \omega_D$ and Λ , the expression simplifies to $D_A^{\text{vertex}} = \Lambda/(\Lambda - \omega_D)$. Note that if we work in the limit where $\Lambda \gg \omega_D$, we have $D_A^{\text{vertex}} = 1$, and we retrieve the result obtained in Appendix A. However, if we work in the opposite limit where $\omega_D \gg \Lambda$, we obtain $D_A^{\text{vertex}} \approx -\Lambda/\omega_D \rightarrow 0$. This agrees with previous work on Kohn-Luttinger corrections that considered static interactions [7,43], which found that the Kohn-Luttinger corrections disappear in the low-density limit ($\mu_c < 0$).

-
- [1] J. Bardeen, L. N. Cooper, and J. R. Schrieffer, *Phys. Rev.* **108**, 1175 (1957).
- [2] A. Karakozov, E. Maksimov, and S. Mashkov, *Zh. Eksp. Teor. Fiz* **68**, 1937 (1975).
- [3] W. Kessel, *Z. Naturforsch. Teil A* **29**, 445 (1974).
- [4] P. Hertel, *Z. Phys. A* **248**, 272 (1971).
- [5] V. Geilikman and N. Masharov, *J. Low Temp. Phys.* **6**, 131 (1972).
- [6] O. V. Dolgov, I. I. Mazin, A. A. Golubov, S. Y. Savrasov, and E. G. Maksimov, *Phys. Rev. Lett.* **95**, 257003 (2005).
- [7] A. V. Chubukov, I. Eremin, and D. V. Efremov, *Phys. Rev. B* **93**, 174516 (2016).
- [8] F. Marsiglio, *Phys. Rev. B* **98**, 024523 (2018).
- [9] R. Combescot, *Phys. Rev. B* **42**, 7810 (1990).
- [10] J. F. Schooley, W. R. Hosler, and M. L. Cohen, *Phys. Rev. Lett.* **12**, 474 (1964).
- [11] J. F. Schooley, W. R. Hosler, E. Ambler, J. H. Becker, M. L. Cohen, and C. S. Koonce, *Phys. Rev. Lett.* **14**, 305 (1965).
- [12] X. Lin, G. Bridoux, A. Gourgout, G. Seyfarth, S. Krämer, M. Nardone, B. Fauqué, and K. Behnia, *Phys. Rev. Lett.* **112**, 207002 (2014).
- [13] I. A. Chernik and S. N. Lykov, *Sov. Phys. Solid State* **23**, 817 (1981).
- [14] Y. Nakajima, R. Hu, K. Kirshenbaum, A. Hughes, P. Syers, X. Wang, K. Wang, R. Wang, S. R. Saha, D. Pratt *et al.*, *Sci. Adv.* **1**, e1500242 (2015).
- [15] O. Prakash, A. Kumar, A. Thamizhavel, and S. Ramakrishnan, *Science* **355**, 52 (2017).
- [16] L. V. Gurevich, A. Larkin, and Y. A. Firsov, *Sov. Phys. Solid State* **4**, 185 (1962).
- [17] Y. Takada, *JPSJ* **49**, 1267 (1980).
- [18] M. Ikeda, A. Ogasawara, and M. Sugihara, *Phys. Lett. A* **170**, 319 (1992).
- [19] C. Grimaldi, L. Pietronero, and S. Strässler, *Phys. Rev. Lett.* **75**, 1158 (1995).
- [20] G. D. Mahan, *Many-Particle Physics* (Springer Science & Business Media, New York, 2000).
- [21] J. M. Edge, Y. Kedem, U. Aschauer, N. A. Spaldin, and A. V. Balatsky, *Phys. Rev. Lett.* **115**, 247002 (2015).
- [22] J. Ruhman and P. A. Lee, *Phys. Rev. B* **94**, 224515 (2016).
- [23] L. P. Gorkov, *Phys. Rev. B* **93**, 054517 (2016).
- [24] L. P. Gorkov, *J. Supercond. Nov. Magn.* **30**, 845 (2017).
- [25] J. Ruhman and P. A. Lee, *Phys. Rev. B* **96**, 235107 (2017).
- [26] D.-H. Lee, *Chinese Phys. B* **24**, 117405 (2015).
- [27] L. Rademaker, Y. Wang, T. Berlijn, and S. Johnston, *New J. Phys.* **18**, 022001 (2016).
- [28] Y. Zhou and A. J. Millis, *Phys. Rev. B* **93**, 224506 (2016).
- [29] Y. Zhou and A. J. Millis, *Phys. Rev. B* **96**, 054516 (2017).
- [30] T. V. Trevisan, M. Schütt, and R. M. Fernandes, *Phys. Rev. Lett.* **121**, 127002 (2018).
- [31] L. Savary, J. Ruhman, J. W. F. Venderbos, L. Fu, and P. A. Lee, *Phys. Rev. B* **96**, 214514 (2017).
- [32] S. E. Rowley, C. Enderlein, J. Ferreira de Oliveira, D. A. Tompsett, E. Baggio Saitovitch, S. S. Saxena, and G. G. Lonzarich, *arXiv:1801.08121*.
- [33] M. Coak, C. R. S. Haines, C. Liu, S. E. Rowley, G. G. Lonzarich, and S. S. Saxena, *arXiv:1808.02428*.
- [34] P. Wölfle and A. V. Balatsky, *Phys. Rev. B* **98**, 104505 (2018).
- [35] M. Sadovsikii, *JETP* **128**, 455 (2019).
- [36] M. Sadovsikii, *JETP Lett.* **109**, 166 (2019).
- [37] A. Aperis and P. M. Oppeneer, *Phys. Rev. B* **97**, 060501(R) (2018).
- [38] F. Schrodli, A. Aperis, and P. M. Oppeneer, *Phys. Rev. B* **98**, 094509 (2018).
- [39] M. Grabowski and L. J. Sham, *Phys. Rev. B* **29**, 6132 (1984).
- [40] J. R. Engelbrecht, M. Randeria, and C. A. R. Sáde Melo, *Phys. Rev. B* **55**, 15153 (1997).
- [41] C. A. R. Sá de Melo, M. Randeria, and J. R. Engelbrecht, *Phys. Rev. Lett.* **71**, 3202 (1993).
- [42] V. Pokrovsky, *Adv. Phys.* **28**, 595 (1979).
- [43] L. Pisani, A. Perali, P. Pieri, and G. C. Strinati, *Phys. Rev. B* **97**, 014528 (2018).
- [44] A. Perali, C. Grimaldi, and L. Pietronero, *Phys. Rev. B* **58**, 5736 (1998).
- [45] M. N. Gastiasoro, A. V. Chubukov, and R. M. Fernandes, *Phys. Rev. B* **99**, 094524 (2019).
- [46] A. Chubukov, N. V. Prokof'ev, and B. V. Svistunov, *Phys. Rev. B* **100**, 064513 (2019).
- [47] P. Chandra, G. G. Lonzarich, S. Rowley, and J. Scott, *Rep. Prog. Phys.* **80**, 112502 (2017).
- [48] P. Coleman, *Introduction to Many-Body Physics* (Cambridge University Press, Cambridge, 2015).
- [49] Y. Wang and A. Chubukov, *Phys. Rev. B* **88**, 024516 (2013).